Hierarchic Shell Model Based on p－Convergence

p－收斂方式에 基礎한 階層要素 쉘 모델

우 광 성*
Woo, Kwang Sung

요 약

p－收斂 有限要素法은 補間函數의 次數 p를 증가시키는 동안 해석하려는 領域의 分割을 固定시키는 有限要素해석의 새로운 접근방법이다. 이 논문에서는 混合寫像함수에 기초한 새로운 p－收斂 階層要素를 이용한 쉘 모델의 컴퓨터 遂行에 초점을 두었다. Pinch Test문제와 원통형 쉘지붕문제를 통해 제안된 쉘 모델의 剛體運動, round－off 오차, 그리고 收斂性등이 검토되었다.

Abstract

The p－version of the finite element method is a new approach to finite element analysis in which the partition of the domain is held fixed while the degree p of approximating piecewise polynomials is increased. In this paper, the focus is on computer implementation of a new hierarchic p－convergence shell model based on blend mapping functions. Its rigid－body modes, round－off error, and convergence characteristics are investigated.

1. Introduction

Assurance of the reliability and accuracy of computed data is fundamentally important in computer aided analysis and design. In this paper, the equation of how to ensure the reliability and accuracy of computed data in engineering computations concerned with analyses of shell structures is addressed. In order to clearly delineate the objective and scope of this paper, some definitions are necessary. First, we must distinguish between convergence process in finite element analysis. In the conventional finite element convergence process, which we shall call h－convergence, the number and type of the interpolating functions over each element are fixed and the finite element mesh is refined in such a way that the maximum diameter of the elements, h, approaches zero. In the second convergence process, to which we shall refer as p－convergence, the number and distribution of finite elements is fixed and the number of

*정회원, 전남대학교 토목공학과 전임강사, 공학박사

이 논문에 대한 토론을 1990년 9월 30일까지 본 학회에 보내주시면 1991년 3월호에 그 결과를 게재하겠습니다.

basis functions, which are necessarily locally complete polynomials of order p, is progressively increased. [1, 2]

This paper is concerned with p-convergent finite element software systems and the displacement formulation. The development of such software systems has been made possibly by three recent developments. [3, 4]

1. Hierarchic families of finite element, based on the displacement formulation, have been developed.

2. It has been established that whenever h-convergence occurs, p-convergence will also occur, (and vice versa) and the rate of p-convergence cannot be slower than the rate of h-convergence, when h-convergence is based on uniform mesh refinement.

3. Subastantial computational experience has been accumulated which indicates that uniform p-convergent finite element approximations are superior in efficiency to uniform h-convergent approximations.

As early as in 1969 [5], elements with hierarchic characteristics were used, unconciously, in modeling rotational shell elements. The idea of hierarchic finite elements was first suggested by Zienkiewicz et. al. [6] in order to join F.E. with different polynomial degrees. A new and useful family of hierarchic finite elements has been developed by Peano et. al. [7] Hierarchic finite elements have the property that shape functions corresponding to an element of order p consitute a subset of the shape functions of all higher order hierarchie elements of same kind. In other word, when increasing the order of FE, the previous shape functions of the low order element shall be retained. Therefore, it is similar to the Ritz method in an element sense. There are different ways constructing hierarchic sequences of shape functions. However, it is possibe to construct a set of shape functions to give a strongly diagonal element stiffness matrix. [8]

With the hierarchic degrees of freedom appearing as perturbations on the original solution rather than its substitute, one can expect the hierarchic element to have a more diagonal dominant form than that obtainable in a direct approximation involving the identical number of non-hierarchic degrees of freedom. Furthermore, a set of shape functions which can cause an almost diagonal element stiffness matrix can be obtained by the use of the orthogonality property of the Legendre' polynomials. Therefore, this has important consequences of ensuring an improved conditioning of the stiffness matrix and a faster rate of iteration convergence that would be possible with non-hierarchic forms. The hierarchic elements make it easy to use finite elements of different polynomial order. The continuity between elements with different polynomial order is achieved by assigning zero higher order derivatives. Thus along the inter-element boundary, the higher order of approximation is degraded to the lower. [4, 7] This hierarchic nature can lead to the numerical stability and computational efficiency.

In the conventional h-version, there are three distinct approaches to the finite element representation of thin shell structures: (i) in "faceted" form with flat elements, (ii) by means of degenerated three-dimensional solid elements, and (iii) with curved elements formulated on the basis of curved shell theory. The shortcomings and associated difficulties of "those" elements are well known.

Corresponding to the six displacement components of a cylindrical shell, that is u, v, w θ_x, θ_y, θ_z. there should be six rigid-body modes which can be detected by zero-eigenvalue test,

and hence the element stiffness matrix should have six zero eigenvalues related to these modes. The strain-displacement relationships are based on Reissner-Mindlin theory, and hence it may be noted that the aforementioned elements include the effect of transverse shear deformation.

2. Hierarchic Shell Element

2.1 Integrals of Legendre' Polynomials

If the computations could be carried out with unlimited precision, the quality of F.E. approximation would have depended only on the degree of the polynomial used and not how the polynomial shape functions are constructed. On a digital computer, however, the computations can be performed with limited digits of accuracy, and hence each of numerical stability caused by round-off error may become a problem. In order to reduce round-off errors and numerical instability, it is necessary to construct the shape functions appropriately. Therefore, there is no unique optimal set of element shape functions except from considerations of round-off and numerical stability.

The shape functions used in this study are based on the Integrals of the Legendre' polynomials. [9, 10] The Legendre' polynomials are defined by the Rodrigues formula:

$$P_n(x) = \frac{1}{2^n n!}\frac{d^n}{dx^n}(x^2-1)^n \quad n = 0,1,2,.. \qquad (1)$$

with the orthogonality property:

$$\int_{-1}^{1} P_n(t)P_m(t)dt = \begin{cases} 0 & ; \ n \neq m \\ 2/2n+1 & ; \ n = m \end{cases} \qquad (2)$$

The internal modes of 1-D elements, the side modes of 2-D elements and the edge modes of 3-D elements can be defined as follows

$$F_n(x) = \frac{\sqrt{2n-1}}{2}\int_{-1}^{x} P_{n-1}(t)dt \qquad (3)$$

The stiffness matrix resulting from these orthogonal shape functions for the 1-D problem has the condition number 1, i.e., the off-diagonal terms are all zero and the diagonal terms are 1 therefore no digits are lost in solution. For the 2-D case, $F(\xi)$ and $F(\eta)$ are multiplied by the factors $(\eta-1)$, $(\xi+1)$, $(\eta+1)$, $(\xi-1)$ for sides 1 through 4 respectively in order to obtain sequence of hierarchic shape functions.

Table 1. Shape functions for side 1 of Legendre' quadrilateral element

P-Level	$F(\xi,\eta)$
2	$\frac{3}{2\sqrt{6}}(\eta+1)(\xi^2-1)$
3	$\frac{5}{2\sqrt{10}}(\eta+1)\xi(\xi^2-1)$
4	$\frac{1}{8\sqrt{14}}(\eta+1)(35\xi^4-42\xi^2+7)$
5	$\frac{1}{8\sqrt{18}}(\eta+1)(63\xi^5-90\xi^3+27\xi)$
6	$\frac{1}{16\sqrt{22}}(\eta+1)(231\xi^6-385\xi^4+165\xi^2-11)$
7	$\frac{1}{16\sqrt{26}}(\eta+1)(429\xi^7-819\xi^5+455\xi^3-65\xi)$
8	$\frac{1}{128\sqrt{30}}(\eta+1)(6435\xi^8-13860\xi^6+9450\xi^4-2100\xi^2+75)$
9	$\frac{1}{128\sqrt{34}}(\eta+1)(12155\xi^9-29172\xi^7+23562\xi^5-7140\xi^3+595\xi)$
10	$\frac{1}{256\sqrt{38}}(\eta+1)(46189\xi^{10}-122265\xi^8+114114\xi^6-43890\xi^4+5985\xi^2-133)$

Table 2. Internal Modes of Legendre' Quadrilateral Element

polynomial degree	$F(\xi,\eta)$
4	$F_2(\xi)F_2(\eta)$
5	$F_3(\xi)F_2(\eta)$ $F_2(\xi)F_3(\eta)$
6	$F_4(\xi)F_2(\eta)$ $F_3(\xi)F_3(\eta)$ $F_2(\xi)F_4(\eta)$
7	$F_5(\xi)F_2(\eta)$ $F_4(\xi)F_3(\eta)$ $F_3(\xi)F_4(\eta)$ $F_2(\xi)F_5(\eta)$
8	$F_6(\xi)F_2(\eta)$ $F_5(\xi)F_3(\eta)$ $F_4(\xi)F_4(\eta)$ $F_3(\xi)F_5(\eta)$ $F_2(\xi)F_6(\eta)$
9	$F_7(\xi)F_2(\eta)$ $F_6(\xi)F_3(\eta)$ $F_5(\xi)F_4(\eta)$ $F_4(\xi)F_5(\eta)$ $F_3(\xi)F_6(\eta)$ $F_2(\xi)F_7(\eta)$
10	$F_8(\xi)F_2(\eta)$ $F_7(\xi)F_3(\eta)$ $F_6(\xi)F_4(\eta)$ $F_5(\xi)F_5(\eta)$ $F_4(\xi)F_6(\eta)$ $F_3(\xi)F_7(\eta)$ $F_2(\xi)F_8(\eta)$

Side modes of the rectangular element are given in Table 1 for polynomial degree 1 through 10. In order to satisfy the completeness requirement, internal modes, also called "bubble modes", given in Table 2, must be introduced. The internal modes can be formed as the product of the $F_m(\xi)$ and $F_n(\eta)$ for a ll m and n such that $m+n=p$, $m,n>2$. The stiffness matrix constructed for the cylindrical shell problem using Legendre' polynomials as shape functions will not be exactly orthogonal as in the case of 1-D problem but it will remain "nearly orthogonal", i.e. the diagonal terms will dominate for reasons stated earlier.

2.2 Blend Mapping

In order to conform better suited to curved geometries and reduce discretization error, curved finite elements have been widely used in recent years. The most well known of such elements are the parametric (iso- or sub-) family of elements. For mathematical convenience, in general, the shape functions are defined on the standard domains (e.g. triangles, squares, cubes, etc.) and are mapped into the real domain by suitable coordinate transformations. The most commonly used mappings are linear and quadratic parametric mappings which have served the h-version well. This is because, in general, the mapping does not introduce large distortions in the h-version, and all piecewise smooth boundaries can be approximated by a sufficient number of piecewise quadratic polynomials.

In the p-version, the size of elements is usually large and hence the probability of distortions is more, especially if higher order parametric mapping is used, unless the boundary of an element is represented by a polynomial in the parametric form. In the case of non-polynomial boundaries, like circles and ellipses, parametric mapping may not work at all. In the case of proposed element, only the four corners of a quadrilateral element will be referred to in mapping from the standard to real domain.It is therefore necessary to find mapping function which will exactly map the standard element to the sides of the real element including the four corner nodes by making use of the exact geometric parameters of the curved boundaries shown in Fig. 1 with the help of transfinite interpolants. This can be achieved by constructing blend mapping functions. [11] As a special case, the mapping function for an element bounded by lines $x=$const. and $\theta=$const. can be expressed as:

$$x = \sum_{k=1}^{4} M_k(\xi,\eta)x_k$$

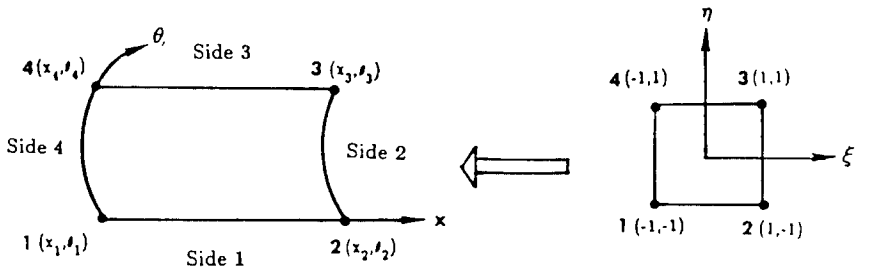

Fig. 1 Blend mapping from standard domain to real domain

$$\theta = \sum_{k=1}^{4} M_k(\xi,\eta)\theta_k \tag{4}$$

where $M_k(\xi,\eta) = \frac{1}{4}(1+\xi\xi_k)(1+\eta\eta_k)$.

2.3 Element stiffness matrix

The strain energy of the k−th element is of the form (5)

$$U_k = \frac{1}{2}\int_{\Omega_k} (\{D\}\{u\})^T [E]\{D\}\{u\}\,dA,$$

In the case of cylindrical shell, the strain matrix is expressed as :

$$\{D\} = \begin{bmatrix} \frac{\partial}{\partial x} & 0 & 0 & 0 & 0 \\ 0 & \frac{\partial}{R\partial\theta} & \frac{1}{R} & 0 & 0 \\ \frac{\partial}{R\partial\theta} & \frac{\partial}{\partial x} & 0 & 0 & 0 \\ 0 & 0 & 0 & \frac{\partial}{\partial x} & 0 \\ 0 & 0 & 0 & 0 & \frac{\partial}{R\partial\theta} \\ 0 & 0 & 0 & \frac{\partial}{R\partial\theta} & \frac{\partial}{\partial x} \\ 0 & 0 & \frac{\partial}{\partial x} & 1 & 0 \\ 0 & \frac{-1}{R} & \frac{\partial}{R\partial\theta} & 0 & 1 \end{bmatrix} \tag{6}$$

[E] which is the material stiffness matrix, for an elastic isotropic material, in the absence of initial stresses and strains, can be expressed as:

$$[E] = \begin{bmatrix} K_1 & K_2 & 0 & 0 & 0 & 0 & 0 & 0 \\ K_2 & K_1 & 0 & 0 & 0 & 0 & 0 & 0 \\ 0 & 0 & K_3 & 0 & 0 & 0 & 0 & 0 \\ 0 & 0 & 0 & D_1 & D_2 & 0 & 0 & 0 \\ 0 & 0 & 0 & D_2 & D_1 & 0 & 0 & 0 \\ 0 & 0 & 0 & 0 & 0 & D_3 & 0 & 0 \\ 0 & 0 & 0 & 0 & 0 & 0 & S_1 & 0 \\ 0 & 0 & 0 & 0 & 0 & 0 & 0 & S_1 \end{bmatrix} \tag{7}$$

where

$$K_1 = \frac{Et}{1-\nu^2}, \qquad K_2 = \nu K_1$$

$$K_3 = \tfrac{1}{2}(1-\nu)K_1, \qquad D_1 = \frac{Et^3}{12(1-\nu^2)}$$

$$D_2 = \nu D_1, \qquad D_3 = \frac{1-\nu}{2} D_1$$

$$S_1 = \frac{Et}{2(1+\nu)\alpha}; \qquad \alpha = 6/5.$$

After the shape functions are substituted into matrix [B], the element stiffness matrix can be evaluated from eqn (5). A typical submatrix of $[K^e]$ linking nodes i and j can then be evaluated with the expression

$$[\mathbf{K}_{ij}^e] = \int\int [\mathbf{B}_i]^T [\mathbf{D}][\mathbf{B}_j]\, dA$$

in which

$$dA = R\, d\theta\, dx = R \det \mathbf{J}\, d\xi\, d\eta$$

$\det \mathbf{J}$ = determinant of the Jacobian matrix.

3. Computer Implementation

3.1 Round−off Error

The susceptibility of a matrix to round−off errors in the solution of simultaenous equation is characterized by the condition number(CN). It can be shown that the maximum number of digits lost in numerical operations involving

a given matrix is not greater than LOG(CN). As a result, the shape functions that perform better numerically are the ones that will result in a stiffness matrix that has a smaller condition number. In general, the stiffness matrix [K] will be ideally well-conditioned if CN is close to one and ill-conditioned when CN is significantly greater than one. In order to calculate the condition number of the stiffness matrix one has to calculate the largest and smallest eigenvalues of Eq. (8).

$$([K]-\lambda[I])\ \{u\}=0 \tag{8}$$

The condition number can then be defined as [12]:

$$CN=\frac{|\lambda max|}{|\lambda min|} \tag{9}$$

According to Ref. [12], very thin shell may yield $CN=10^{12}$ because its membrane stiffness is much greater than its bending stiffness. If the diameter-to-thickness ratio of a shell is 1000, the condition number may exceed 10^{15} by h-version model. On the other hand, in the case of shell elements developed herein the variation of the loss of significant digits with p-level are shown in Fig.2 with radius=4.953 in., Poisson's ratio=0.3125, Young's modulus=10.5×10^6 psi, central angle of shell element=90°, and R/t ratios of 16.5, 52.69, and 319.96. It can be seen that the maximum number of digits lost which can be difined by LOG(CN) lies between 2 for p=1 to 5,6 or 7 for thick, thin and very thin shell when p=8. It may be noted that for p>2, number of digits lost remains virtually unchanged.

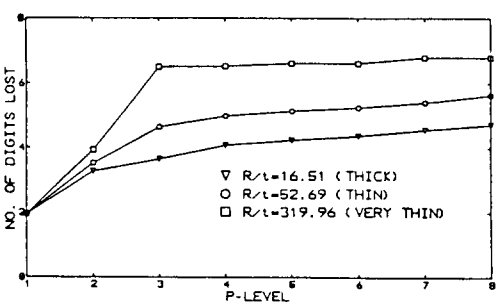

Fig. 2 Condition Number of cylindrical shell elements : (R=4.953 in, $\nu=0.3125$, $E=10.5\times10^6$ psi, and central angle of shell element=90°)

3.2 Rigid-Body Motion

The eigenvalue test can detect zero-energy modes, lack of invariance, and other defects. It is one of several tests of element quality. If each eigenvector $\{u_i\}$ is normalized so that $\{u_i\}^t\{u_i\}=1$, Eq. (8) yields

$$\lambda_i=\{u_i\}^t[K]\{u_i\}=2U_i \tag{10}$$

Thus each eigenvalue λ_i of [K] is twice the element strain energy U_i when (normalized) nodal displacement $\{u_i\}$ are imposed. One can find λ_i when the corresponding $\{u_i\}$ represents rigid-body motions---translation or rotation, singly or in combination. There are three linearly independent rigid-body modes for a plane element and six for a shell element. Table 3 shows first nine eigenvalues for a cylindrical

Table 3. Zero Eigenvalues of Cylindrical Shell Element with P=8

	Eigenvalue
λ_1	0.77594E-10
λ_2	0.56157E-09
λ_3	0.36391E-09
λ_4	0.42362E-02
λ_5	0.79867E-04
λ_6	0.18612E-09
λ_7	0.32015E+02
λ_8	0.35772E+02
λ_9	0.39425E+02
λ_{max}	0.13918E+08

shell element modelled by a quarter cylinder with R=4.953 in and t=0.094 in. It is shown that the first six eigenvalues are small enough to be treated as zero comparing to the remaining eigenvalues. Hence the porposed elements satisfy the rigid-body motion requirements. [12]

4. Numerical Results

4.1 Pinched Cylindrical Shell

Two problems are considered, one a thin shell with R/t=53, and the other a very thin shell R/t=320. The first shell was analyzed by Bogner et al. [13] Recently this problem was solved by Hansen and Heppler [14] and Carpenter et al. [15] It has a radius of 4.953 in, a thickness of 0.094 in, and a pinch load of 100 lb. The second shell has the same radius as the first but its thickness is taken as 0.01548 in, and its pinch load is 0.1 lb. For both shells, the Young's modulus is taken as 10.5×10^6 psi and Poisson's ratio as 0.3125. Because of the symmetry only one octant of shell, as shown in Fig. 3, is considered.

In the case of the first shell the radial deflection under the point load based on thin shell equations is 0.1084 in by Timoshenko and Woinowsky-Krieger. An ABAQUS solution based on a [5×5] mesh of S8R elements is found to be 0.1135 in. and with a [10×10] mesh of S4R elements the value is 0.1115 in [16] The results for this problem published by different authors and present study by the p-version are shown in Table 4.

The importance of rigid-body modes is evident from the results of Cantin and Clough [17] with a [3×49] mesh. A deflection of 0.11 28 in was obtained by them when the rigid-body modes were included and the value was 0.0558 in. when the rigid-body modes were excluded. The p-version result is 0.1126 in with a single eigth-order element. Table 5 shows the deflection(inch) under the pinch load for the very thin pinched cylinder problem. The best available analytical result is 0.0244 in by Ashwell and Gallagher. [18] An ABAQUS solution based on a [5×5] mesh of S8R elements is found to be 0.0245 in and with a [10×10] mesh S4R elements 0.0241 in. The p-version result with a single eigth-order element(NDOF=110) is 0.0244 in.

The convergence characteristics of maximum deflection and total potential energy for a single element model of the thin cylinder, as the p-level is increased from 4 to 9, are shown in Figs. 4 and 5. with just one element the results appear to converge at a p-level of 6. The effect of mesh refinement, keeping the p-level fixed at 5, is shown in Table 6.

The meshes used for this purpose are graded toward the point load, as shown in Fig. 3. With one element and p=9, the maximum deflection is 0.1130 in. Whereas in Table 6 the graded 4-element model with p=5 gives a value as 0.1134 in. Therefore, a graded mesh with sufficiently high p-level leads to better results with somewhat fewer degrees of freedom.

To achieve the same degree of accuracy, the CPU time requirements of p-version solution with one element was found to be 13.86 sec as compared to 29.43 sec with ABAQUS based on [10×10] S4R model and 26.69 sec by [5×5] S8R element. These runs were made on a VAX-8800 computer. It is expected that more spectacular savings in CPU time can be achieved with p-version if more efficient equation solver and quadrature algorithm are used. It is worthwhile to note that to achieve the same level of accuracy, a single fifth-order element req-

uires 13.86 sec of CPU time whereas 49 quadratic elements require 65.77 sec of CPU time when both runs are made with the p-version of F.E. program, SHLPV.

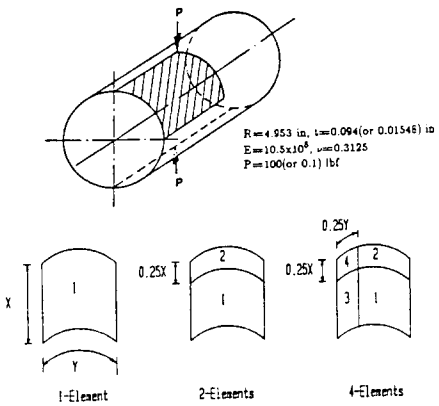

Fig. 3 An octant of pinched cylinder problem and mesh refinement

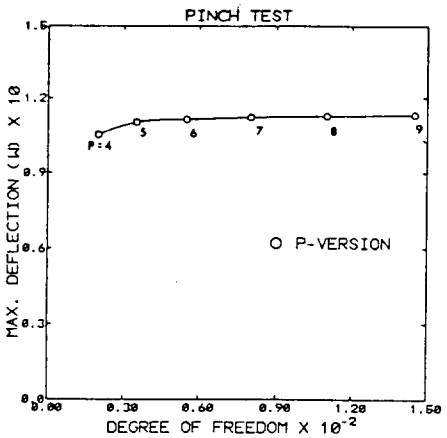

Fig. 4 Convergence of p-level & NDOF vs. Wmax

Table 4. Deflection(inch) under point load for thin pinched cylinder problem

Mesh	Cantin (1970)	Ashwell and Sabir (1972)	Thomas and Gallagher (1975)	Bogner *et al.* (1967)	Mesh	Cantin and Clough (1968)
1×1		0.104(20)	0.0048(19)	0.0025(48)		
1×2				0.0802(72)	1×3	0.0297(48)
1×4		0.1106(50)	0.1107(67)	0.1087(120)	1×5	0.0769(72)
1×8			0.1119(131)		1×7	0.0987(96)
2×2	0.0931(54)	0.1103(45)		0.0808(108)	1×9	0.1057(120)
4×4	0.1126(150)	0.1129(125)			2×9	0.1073(180)
6×6	0.1137(294)	0.1135(245)			3×49	0.1128(1200)
8×8	0.1139(486)	0.1137(405)				
10×10	0.1139(726)	0.1137(605)				
5×5	0.1135(390) ABAQUS S8R element					
10×10	0.1115(540) ABAQUS S4R element					
1×1	0.1126(110) $p = 8$ by p-version					
2×2	0.1134(125) $p = 5$ by p-version					

Figures in parentheses give *NDOF*.

4.2 Barrel Vault

The barrel vault problem shown in Fig. 6 is generally treated as a test problem to study the performance of shell elements. It is loaded by its own weight in the z-direction. The cylindrical shell is supported by diaphragms at the ends. The diaphragm prevent in the y- and z-directions but allow displacement in the x-direction. Poisson's ratio is zero and modulus of elasticity is 3.0×10^6 psi. Because of two planes of symmetry, it is sufficient to discretize only one quarter of the shell. The goal of computation is to compute displacements, mem-

Table 5. Deflection(inch) under point load for very thin pinched cylinder problem

Mesh	Ashwell and Sabir (1972)	Thomas and Gallagher (1975)	Cantin and Clough (1968)	Sabir and Lock (1972)
1 × 1	0.2301(20)	0.00003(19)	0.00001(24)	0.00001(20)
1 × 2		0.01582(35)		
1 × 4	0.02403(50)	0.02327(67)	0.00074(64)	0.00063(50)
1 × 6		0.02440(99)		
1 × 8	0.02406(90)	0.02467(131)	0.00700(108)	0.00691(90)
2 × 8	0.02414(135)		0.00699(162)	0.00694(135)
3 × 8	0.02418(180)		0.00699(216)	0.00696(180)
8 × 8	0.02431(405)		0.00708(486)	0.00706(405)
5 × 5	0.02453(390) ABAQUS S8R element			
10 × 10	0.02405(540) ABAQUS S4R element			
1 × 1	0.02441(110) p = 8 by p-version			

Figures in parentheses give *NDOF*.

Table 6. Results of mesh refinement with p=5

Number of mesh elements	*NDOF*	P.E.	W_{max} (in.)
1	34	−0.138E+1	0.110131
2	70	−0.139E+1	0.111125
4	125	−0.142E+1	0.113417

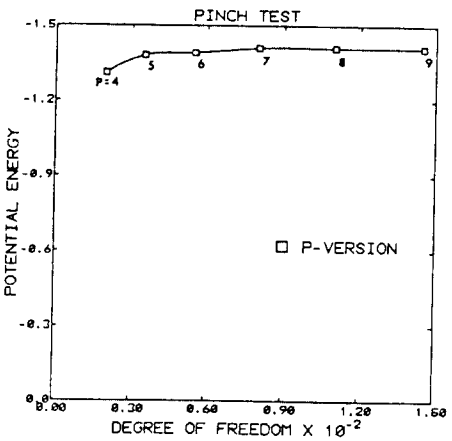

Fig. 5 Convergence of NDOF vs. Potential Energy

brane forces and moments at selected points about one percent relative error.

The history of the solution of this problem is rather involved. The first authors to quote a solution appear to be Cantin and Clogh [17] who used a program described by Scordelis. Many authors quote the program described by Scordelis and Lo. [19] Although the value the vertical deflection at the center of a free edge as 3.696 in, whereas Cowper, Lindberg and Olson give the value 3.7033 in. [20]

The exact analytical solution based on the shallow shell formulation is 3.7033 in and for the deep shell formulation is 3.59 in. ABAQUS's S4R element yields 3.629 in when 2166 degrees of freedom are used. Curiously enough, in a paper from Washington University in 1988 [21], an attempt has been made to solve the above problem using from 3−D hierarchic elements of 8th order. The weight of the shell was represented as equal tractions on the outer and inner surfaces. Thus with 1436 degrees of freedom the maximum deflection is reported to be 3.613 in. Results are also presented for four element hierarchic shell model with p=1 2, q=1 and NDOF=1728, leading to a deflection of 3.616 in. The loading in this work is approximated by uniformly distributed traction.

But the results obtained by SHLPV using one eighth order element is 3.6318 in, one ninth order element is 3.6430 in and one tenth order element is 3.6664 in when ν=0.0. The comparative results with the hierarchic shell model

of Washington University are shown in Table 7. The nodal displacement along BC is plotted in Fig. 7 in comparison with the results based on Donnel-Jenkins' classical theory. Also the bending moments along BC are plotted in Figs. 8, 9.

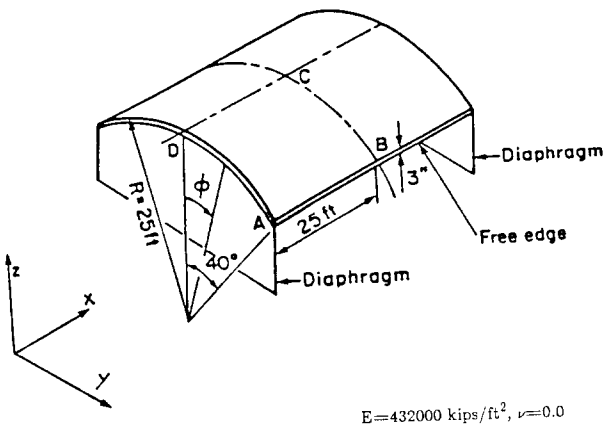

E=432000 kips/ft^2, ν=0.0

gravity load=0.09 kips/ft^2

Fig. 6 Simple shell segment under gravity load

Table 7. Computed values of normal displacement(inch) by hierarchic shell model of Washington University & SHLPV

Hierarchic Shell Model Washington Univ. (4-elements)			SHLPV Vanderbilt Univ. (1-element)		
p,q	NDOF	$(w)_{at\ B}$	p	NDOF	$(w)_{at\ B}$
4,1	224	3.606	6	55	3.5989
6,1	456	3.611	7	80	3.6140
8,1	784	3.613	8	110	3.6318
10,1	1208	3.615	9	145	3.6430
12,1	1728	3.616	10	185	3.6664

5. Summary and conclusions

The present state of development of a new hierarchic shell elements with high order using exact blend mapping that satisfies all the requirements of constant strains and rigid-body modes has been reviewed. In this procedure,

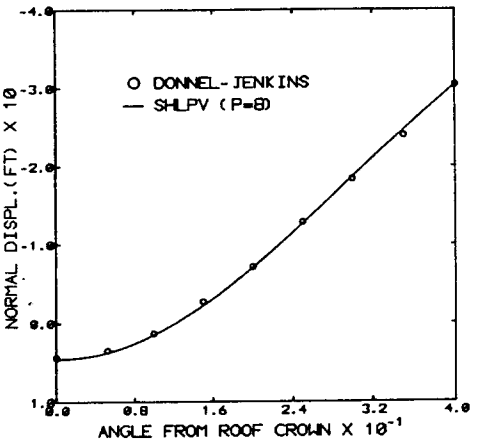

Fig. 7 Normal dispacement w along BC of shell roofs

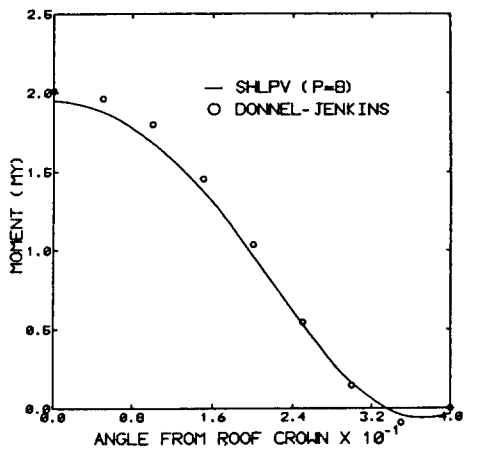

Fig. 8 Bending moment My along BC of shell roofs

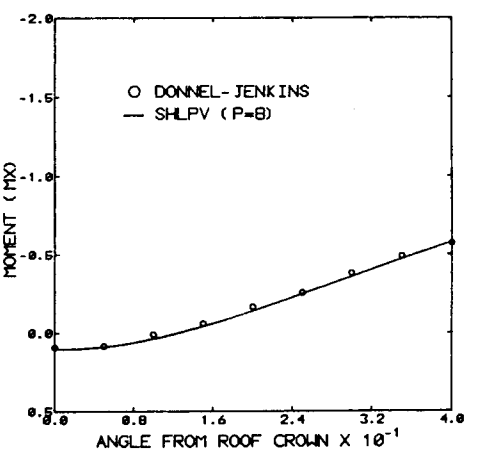

Fig. 9 Bending moment Mx along BC of shell roofs

the finite element mesh is fixed and the number or type of basis functions is varied over the mesh, either uniformly or selectively, until some desired level of precision is reached. The basis functions are complete polynomials, which are hierarchic, i.e. the set of basis functions associated with each higher order element of the same kind. Consequently, the stiffness matrix based on the proposed element is well-conditioned even when very high levels of p are used. There are several computational advantages, the most important of which are that the rate of convergence is much faster than the rate of convergence achieved through mesh refinement. The proposed p-convergence shell model is therefore a worthy alternative to the existing cylindrical shell element.

6. References

1. P.K. Basu, M.P. Rossow, B.A. Szabo, " Technical Documentation and User's Manual : COMET-X" Report No. R-340, Federal Railroad Adminitration, Aug. 1977
2. P.K. Basu, R.M. Lamprecht, "Some Trends in Computerized Stress Analysis", Proc. of Seventh ASCE Conference in Electronic Computation, Washington University, Aug. 1979.
3. B.A. Szabo, "Some Recent Developments in Finite Element Analysis", Comp. Math. Applications, 5, pp. 99-115, 1979.
4. I. Babuska, B.A. Szabo, "On the Rates of Convergence of the Finite Element Method", Int. J. Numer. Meth. Eng., Vol. 18, pp. 323-341, 1982.
5. L.J. Brombolish, P.L. Gould, "Finite Element Analysis of Shells of Revolution by Minimization of the Potential Energy Functional", Proc. of the Symposium on Application of Finite Element Methods in Civil Eng., Vanderbilt University, ASCE, pp. 279-307, 1969.
6. O.C. Zienkiewicz, B.M. Irons, F.C. Scott, J. Campbell, "Three Dimensional Stress Analysis", Proc. INTAM Symp. On High Speed Compuing of Elastic Structure, pp. 413-433, 1971.
7. A.G. Peano, "Hierarchies of Conforming Finite Elements for Plane Elasticity and Plate Bending", Comp. Math. Applications, Vol 2, pp. 211-224, 1976.
8. O.C. Zienkiewicz, J.P. De S.R. Gago, D.W. Kelly, "The Hierarchical Concept in Finite Element Analysis", Computers & Structures, Vol 16, pp. 51-65, 1983.
9. P.K. Basu, "Dimensional Reduction of Structural Plates and Shells", NSF Research Report, Grant No. CEE-84115675, Vanderbilt University, 1986.
10. K.S. Woo, "High precision analysis of plates and cylindrical shells in the presence of singularities by the p-version of the finite element method", Ph.D. Dissertation, Vanderbilt University, 1988.
11. W.J. Gordon, C.A. Hall, "Transfinite Element Methods : Blending Function Interpolation over Arbitrary Curved Element Domains", Numer. Math. 21, pp. 109-129, 1973.
12. R.D. Cook, "Concepts and Applications of Finite Element Analysis", Second Edition, John Wiley & Sons, New York, 1981.
13. F.K. Bogner, R.L. Fox, L.A. Schmit, "A cylindrical shell discrete element", AIAA J. 5, 745, 1967.
14. J.S. Hansen, G.R. Heppler, "A Mindlin shell element that satisfies rigid-body requirements", AIAA J. 23(2), 288-295, 1985
15. N. Carpenter, H. Stolarski, T. Belytschko, "Improvement in 3-node triangular shell

elements", Int. J. Numer. Meth. Eng. 23, pp. 1643-1667, 1986.
16. Hibbitt, Karlsson and Sorensen, Inc. ABAQUS Example Problems Manual, 1985.
17. G. Cantin, R.W. Clough, "A curved cylindrical shell, finite element", AIAA J. 6(6), 1057-1062, 1968.
18. D.G. Ashwell, R.H. Gallagher, "Finite Elements for Thin Shells and Curved Members", John Wiley & Sons, New York, 1976.
19. A.C. Scordelis, K.S. Lo, "Computer analysis of cylindrical shells", J. Am. Concr. Inst. 61, 539-561, 1964.
20. G.R. Cowper, G.M. Lindberg, M.D. Olson, "A shllow shell finite elements of triangular shape", Int. J. Solids Struct. 6, 1133-1156, 1970.
21. B.A. Szabo, G.J. Sahrmann, "Hierarchic Plate and Shell Models Based on p-Extension", Int. J. Numer. Meth. Eng. Vol. 26, 1855-1881, 1988.

(접수일자 : 1990. 2. 8)